Electronic Supporting Information

# Construction of three new Co(II)-organic frameworks based on diverse metal clusters :highly selective $C_2H_2$ and $CO_2$ capture and magnetic properties

Xian-Feng Sun,[a] Jing-Jing Chen,[a] Dan Gao,[a] Li-Na Zheng,*[a] Bin Liu,[a] Bo Liu,[b] and Tao Ding*[a]

[a]*School of Environmental and Chemical Engineering, Xi'an Polytechnic University, Xi'an 710048, P. R China.*

[b] *College of Chemistry & Pharmacy, Northwest A&F University, Yangling, 712100, P. R. China*

**Table S1. Selected Bond Length (Å) and Angles (°) for 1-3**

| **1** | | | |
|---|---|---|---|
| Co(1)-O(1) | 2.086(3) | Co(1)-O(2) | 2.054(3) |
| Co(1)-O(4) | 2.153(5) | Co(1)-O(5)#2 | 2.098(4) |
| Co(1)-O(6)#3 | 2.093(4) | Co(1)-N(1)#4 | 2.202(4) |
| Co(2)-O(2)#5 | 2.049(5) | Co(2)-O(2) | 2.049(5) |
| Co(2)-O(3)#5 | 2.107(3) | Co(2)-O(3)#1 | 2.107(3) |
| Co(2)-O(3)#6 | 2.107(3) | Co(2)-O(3) | 2.107(3) |
| O(1)-Co(1)-O(1)#1 | 180.0 | O(1)#1-Co(1)-O(4)#3 | 91.81(15) |
| O(1)#1-Co(1)-O(4)#2 | 88.19(15) | O(1)-Co(1)-O(4)#3 | 88.19(15) |
| O(1)-Co(1)-O(4)#2 | 91.81(15) | O(1)#1-Co(1)-O(6)#1 | 85.71(17) |
| O(1)#1-Co(1)-O(6) | 94.29(17) | O(1)-Co(1)-O(6)#1 | 94.29(17) |
| O(1)-Co(1)-O(6) | 85.71(17) | O(4)#2-Co(1)-O(6) | 94.23(15) |
| O(4)#3-Co(1)-O(4)#2 | 180.0(3) | O(4)#3-Co(1)-O(6) | 85.77(15) |
| O(4)#3-Co(1)-O(6)#1 | 94.23(15) | O(4)#2-Co(1)-O(6)#1 | 85.77(15) |
| O(6)-Co(1)-O(6)#1 | 180.0 | O(2)-Co(2)-O(3) | 89.16(19) |
| O(2)-Co(2)-O(4)#3 | 109.61(15) | O(2)-Co(2)-O(7)#1 | 92.00(18) |
| O(2)-Co(2)-O(5)#3 | 169.47(15) | O(2)-Co(2)-N(1)#4 | 94.39(15) |
| O(3)-Co(2)-O(4)#3 | 82.47(15) | O(5)#3-Co(2)-O(4)#3 | 59.87(14) |
| O(3)-Co(2)-O(5)#3 | 89.82(18) | O(7)#1-Co(2)-O(3) | 178.70(18) |
| O(7)#1-Co(2)-O(4)#3 | 96.59(15) | O(7)#1-Co(2)-N(1)#4 | 89.02(15) |
| O(7)#1-Co(2)-O(5)#3 | 88.93(17) | N(1)#4-Co(2)-O(3) | 91.46(15) |
| N(1)#4-Co(2)-O(4)#3 | 155.06(14) | N(1)#4-Co(2)-O(5)#3 | 96.12(14) |

Symmetrical codes: #1 -x+1,-y,-z; #2 -x+1/2,y-1/2,-z+1/2; #3 x+1/2,-y+1/2,z-1/2; #4 x,-y+1,z-1/2; #5 -x+1/2,y+1/2,-z+1/2; #6 x-1/2,-y+1/2,z+1/2; #7 x,-y+1,z+1/2 for **1.**

| **2** | | | |
|---|---|---|---|
| Co(1)-O(1) | 2.0263(9) | Co(1)-O(2) | 2.113(3) |
| Co(1)-O(2)#1 | 2.113(3) | Co(1)-O(3)#2 | 2.077(3) |
| Co(1)-O(3)#3 | 2.077(3) | Co(1)-N(1)#4 | 2.182(5) |
| O(1)-Co(1)-O(2) | 93.18(9) | O(1)-Co(1)-O(2)#1 | 93.18(9) |
| O(1)-Co(1)-O(3)#2 | 91.23(9) | O(1)-Co(1)-O(3)#3 | 91.23(9) |
| O(2)-Co(1)-O(2)#1 | 173.65(19) | O(1)-Co(1)-N(1)#4 | 180.0 |
| O(2)-Co(1)-N(1)#4 | 86.82(9) | O(2)#1-Co(1)-N(1)#4 | 86.82(9) |
| O(3)#2-Co(1)-O(2) | 86.52(16) | O(3)#3-Co(1)-O(2) | 93.35(16) |
| O(3)#2-Co(1)-O(2)#1 | 93.35(16) | O(3)#3-Co(1)-O(2)#1 | 86.52(16) |
| O(3)#3-Co(1)-N(1)#4 | 88.77(9) | O(3)#2-Co(1)-O(3)#3 | 177.53(19) |
| O(3)#2-Co(1)-N(1)#4 | 88.76(9) | Co(1)#2-O(1)-Co(1)#6 | 120.0 |
| Symmetrical codes: #1 y-1/3,x+1/3,-z+5/6; #2 -y+1,x-y+1,z; #3 x-y+2/3,-y+4/3,-z+5/6; #4 y,-x+y+1,-z+1; #5 -x+4/3,-x+y+2/3,-z+7/6; #6 -x+y,-x+1,z; #7 x-y+1,x,-z+1 for **2.** | | | |
| **3** | | | |
| Co(1)-O(1) | 2.028(4) | Co(2)-O(2) | 2.045(4) |
| Co(1)-O(1)#1 | 2.028(4) | Co(2)-O(3) | 2.090(4) |
| Co(1)-O(4)#2 | 2.093(4) | Co(2)-O(4)#3 | 2.202(4) |
| Co(1)-O(4)#3 | 2.093(4) | Co(2)-O(5)#3 | 2.164(4) |
| Co(1)-O(6) | 2.124(4) | Co(2)-O(7)#1 | 2.062(4) |
| Co(1)-O(6)#1 | 2.124(4) | Co(2)-N(1)#4 | 2.076(4) |
| O(1)-Co(1)-O(1)#1 | 180 | O(2)-Co(2)-O(3) | 89.16(19) |
| O(1)#1-Co(1)-O(4)#3 | 91.81(15) | O(2)-Co(2)-O(4)#3 | 109.61(15) |
| O(1)#1-Co(1)-O(4)#2 | 88.19(15) | O(2)-Co(2)-O(5)#3 | 169.47(15) |
| O(1)-Co(1)-O(4)#3 | 88.19(15) | O(2)-Co(2)-O(7)#1 | 92.00(18) |
| O(1)-Co(1)-O(4)#2 | 91.81(15) | O(2)-Co(2)-N(1)#4 | 94.39(15) |
| O(1)#1-Co(1)-O(6) | 94.29(17) | O(3)-Co(2)-O(4)#3 | 82.47(15) |
| O(1)#1-Co(1)-O(6)#1 | 85.71(17) | O(3)-Co(2)-O(5)#3 | 89.82(18) |
| O(1)-Co(1)-O(6)#1 | 94.29(17) | O(5)#3-Co(2)-O(4)#3 | 59.87(14) |
| O(1)-Co(1)-O(6) | 85.71(17) | O(7)#1-Co(2)-O(3) | 178.70(18) |
| O(4)#3-Co(1)-O(4)#2 | 180.0(3) | O(7)#1-Co(2)-O(4)#3 | 96.59(15) |
| O(4)#2-Co(1)-O(6) | 94.23(15) | O(7)#1-Co(2)-O(5)#3 | 88.93(17) |
| O(4)#3-Co(1)-O(6) | 85.77(15) | O(7)#1-Co(2)-N(1)#4 | 89.02(15) |
| O(4)#3-Co(1)-O(6)#1 | 94.23(15) | N(1)#4-Co(2)-O(3) | 91.46(15) |
| O(4)#2-Co(1)-O(6)#1 | 85.77(15) | N(1)#4-Co(2)-O(4)#3 | 155.06(14) |
| O(6)-Co(1)-O(6)#1 | 180 | N(1)#4-Co(2)-O(5)#3 | 96.12(14) |
| Symmetrical codes: #1 -x+1, y, z ; #1-x+3/2, -y+3/2, -z+1; #2 -x+1, -y+1, -z; #3 x, -y+1, z ; #4-x+1, y, -z ; #5 -x+2, -y+1, -z+1; #6 -x+2, y, -z+1 for **3.** | | | |

**Table S2.** A comparison of various MOFs materials used for selective adsorption for $C_2H_2$ and $CO_2$ over $CH_4$.

| MOFs materials | IAST calculated selectivity | | Ref. |
|---|---|---|---|
| | $C_2H_2/CH_4$ | $CO_2/CH_4$ | |
| $[(CH_3)_2NH_2][Zn_{1.5}(\mu_3\text{-}O)_{0.5}(F\text{-}tzba)_{1.25}(bpy)_{0.25}(\mu_2\text{-}F)_{0.5}]\cdot 2DMF\cdot 2H_2O$ | 14.4 | 4.2 | 23a |
| $\{[(Me_2NH_2)_{0.5}][Cu_{0.75}(L)_{0.5}(DMA)_{0.375}]\cdot H_2O\}_n$ | | 8.3 | 6a |
| $\{[Cu_4(L)_2(H_2O)_4]\cdot 4DMF\cdot 8H_2O\}_n$ | | 3.2 | 6a |
| $\{[Cu_4(L)_2(ATZ)_2(H_2O)]\cdot 5DMF\cdot 5H_2O\}_n$ | | 7.2 | 6a |
| ZIF-25 | | 2.5 | 16a |
| NOTT-202a | | 1.4 | 23b |
| ZJNU-63 | 13.1 | 3.5 | 24a |
| Sc-ABTC | 14.7 | | 24b |
| $\{[Co_6(\mu_3\text{-}OH)_4(Ina)_8](H_2O)_{10}(DMA)_2\}_n$ | 9.6 | | 23c |
| ZJU-16a | 7.5 | | 24c |
| MOF-505 | ~8.9 | | 24d |
| NOTT-108 | ~6.3 | | 24d |
| HNUST-2 | ~4.3 | | 24d |
| **MOF-2** | 20.1 | 7.6 | This work |
| **MOF-3** | 12.1 | 4.1 | This work |

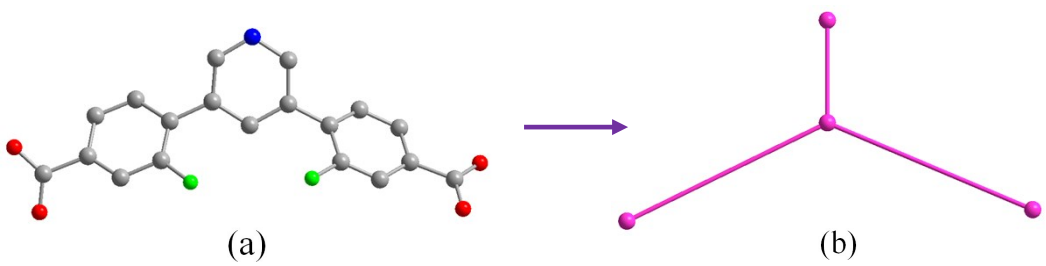


**Figure S1.** The $L^{2-}$ ligand viewed as three kinds of 3-c nodes.

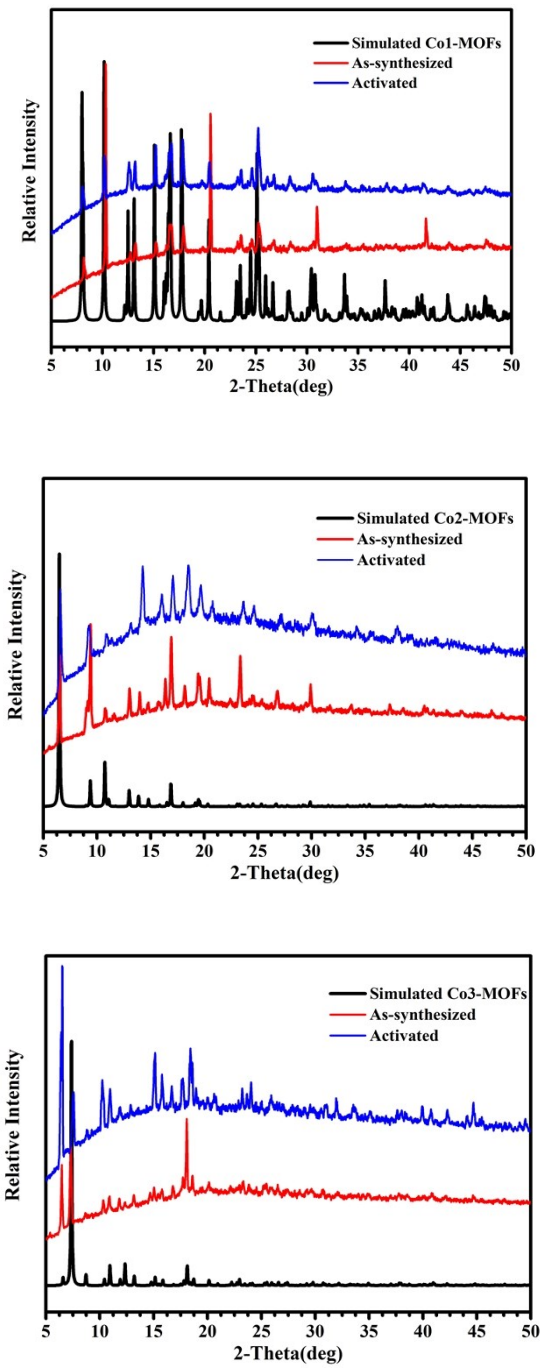


**Figure S2.** PXRD patterns for **1**-**3**: simulated, as-synthesized and activated samples.

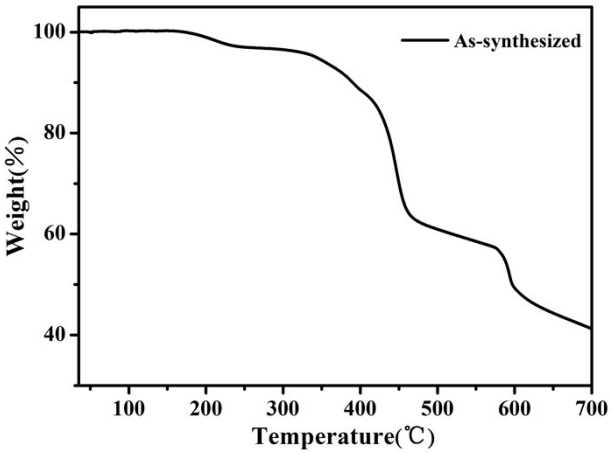


**Figure S3.** TGA for **1**: as-synthesized samples.

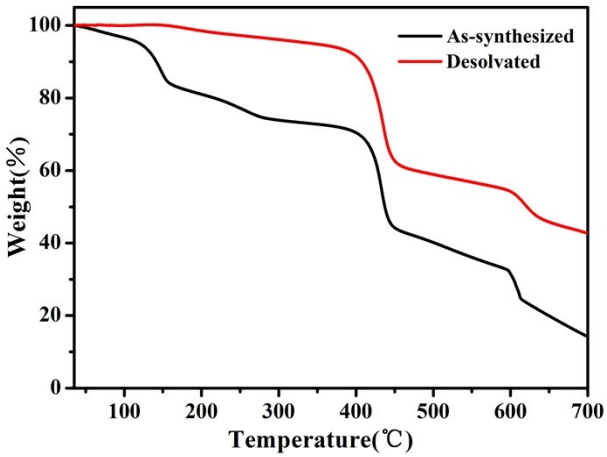


**Figure S4.** TGA for **2**: as-synthesized and desolvated samples.

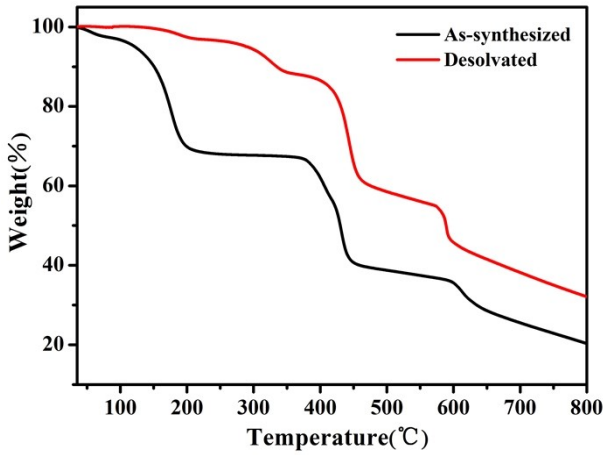


**Figure S5.** TGA for **3**: as-synthesized and desolvated samples.

**IAST adsorption selectivity calculation**

The experimental isotherm data for pure $CO_2$, $CH_4$ and $N_2$ (measured at 298 K) were

fitted using a Langmuir-Freundlich (L-F) model.

$$q = \frac{a * b * p^c}{1 + b * p^c}$$

Where $q$ and $p$ are adsorbed amounts and pressures of component $i$, respectively. The adsorption selectivities for binary mixtures of $CO_2/CH_4$ at 273 and 298 K and $C_2H_2/CH_4$ at 298 K, defined by

$$S_{ads} = (q_1 / q_2) / (p_1 / p_2)$$

Where $qi$ is the amount of $i$ adsorbed and $pi$ is the partial pressure of $i$ in the mixture.

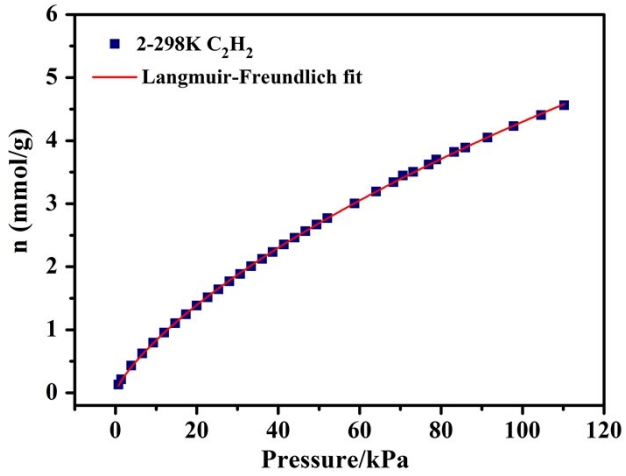


(a)

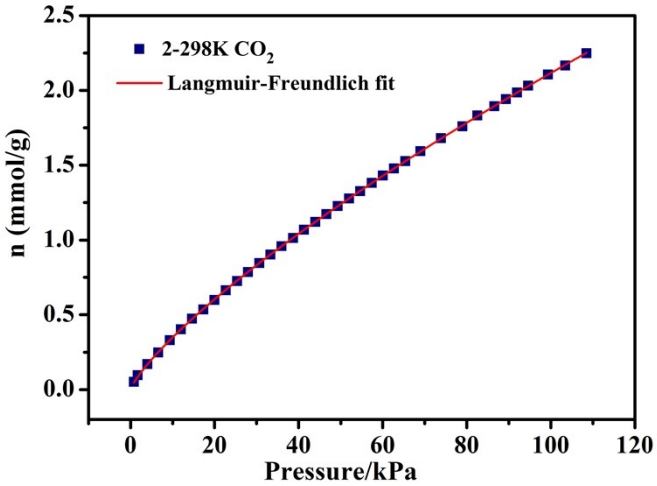


**(b)**

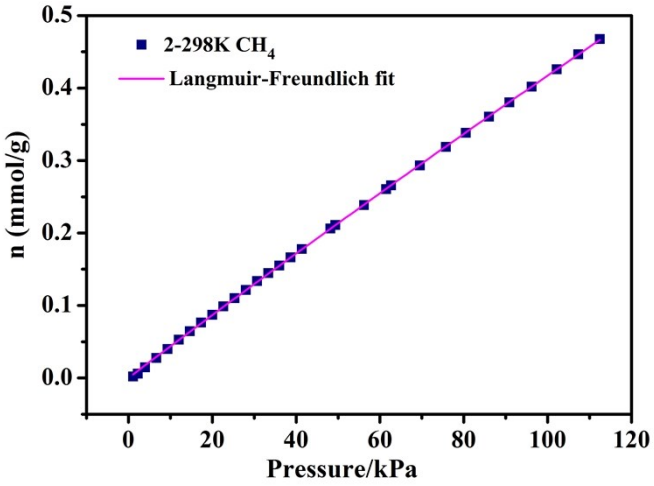


**(c)**

**Figure S6.** (a) $C_2H_2$ adsorption isotherms of **2** at 298 K with fitting by L-F model: a =26.95667, b =0.00533, c =0.22434, Chi^2 = 2.00616E-4, R^2 = 0.99988; (b) $CO_2$ adsorption isotherms of **2** at 298 K with fitting by L-F model: a =40.39902, b =0.00136, c =0.19633, Chi^2 =1.05449E-5, R^2 = 0.99997; (c) $CH_4$ adsorption isotherms of **2** at 298 K with fitting by L-F model: a = 9.68722, b =4.55244, c =0.00252, Chi^2 = 1.70764E-6, R^2 = 0.99992.

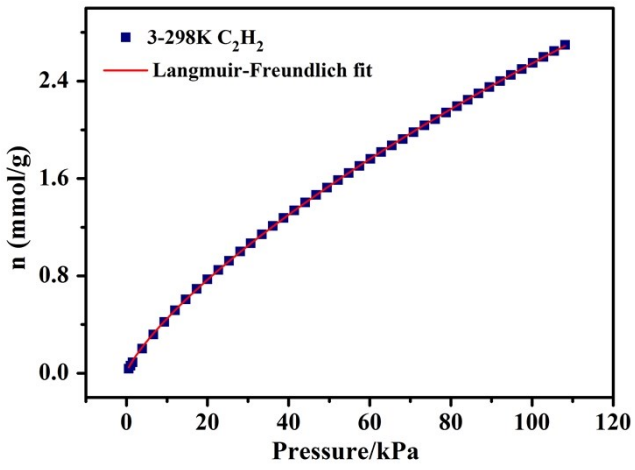


**(a)**

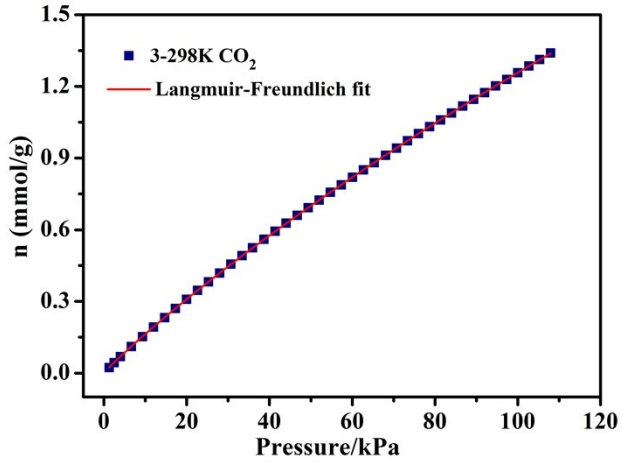


**(b)**

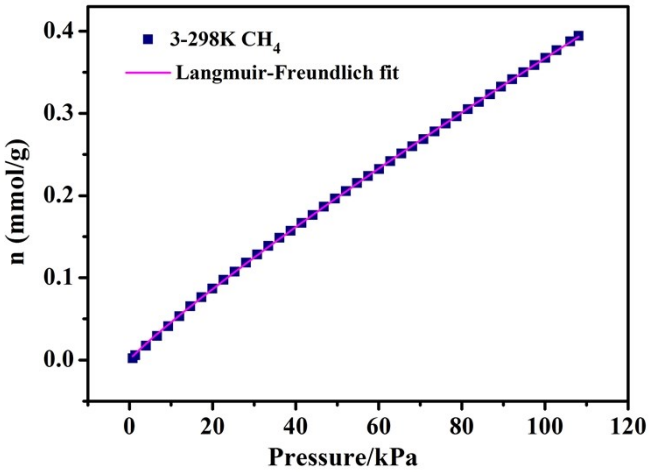


**(c)**

**Figure S7.** (a) $C_2H_2$ adsorption isotherms of **3** at 298 K with fitting by L-F model: a =24.84213, b =0.00331, c =0.1999, Chi^2 = 3.31489E-5, R^2 = 0.99996; (b) $CO_2$ adsorption isotherms of **3** at 298 K with fitting by L-F model: a =9.26861, b =0.00205, c =0.05827, Chi^2 =5.25549E-7, R^2 = 1; (c) $CH_4$ adsorption isotherms of **3** at 298 K with fitting by L-F model: a = 9.70998, b =5.72028E-4, c =0.08157, Chi^2 = 1.19325E-6, R^2 = 0.9999.

**Calculation of sorption heat for $C_2H_2$ and $CO_2$ uptakes using Virial 2 model**

The above equation was applied to fit the combined $C_2H_2$ and $CO_2$ and isotherm data for desolvated **2a** and **3a** at 273 and 298 K, where *P* is the pressure, *N* is the adsorbed amount, *T* is the temperature, *ai* and *bi* are virial coefficients, and *m* and *n* are the number of coefficients used to describe the isotherms. $Q_{st}$ is the coverage-dependent

enthalpy of adsorption and *R* is the universal gas constant.

$$\ln P = \ln N + 1/T \sum_{i=0}^{m} aiN^i + \sum_{i=0}^{n} biN^i Q_{st} = -R \sum_{i=0}^{m} aiN^i$$

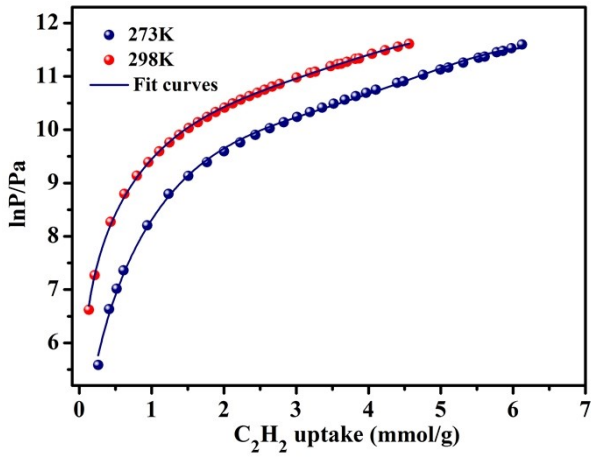


**(a)**

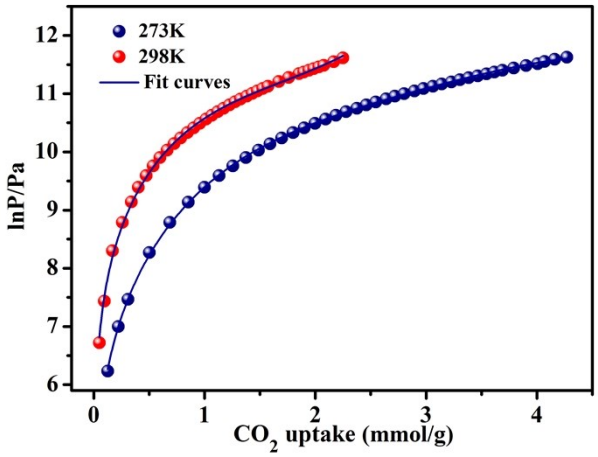


**(b)**

**Figure S8.** (a)Virial analysis of the $C_2H_2$ adsorption data at 298 K and 273 K for **2**. Fitting results: a0= -6794.18492, a1 = 4376.90846, a2 = -1453.97443, a3 =172.82127, a4 = -3.47683, Chi^2 = 0.00618, R^2 = 0.9991; (b) Virial analysis of the $CO_2$ adsorption data at 298 K and 273 K for **2**. Fitting results: a0= -5675.46522, a1 = 1030.50188, a2 = 753.4363, a3 = -343.85346, a4 = -5.75955, Chi^2 = 8.6614E-4, R^2 = 0.9994.

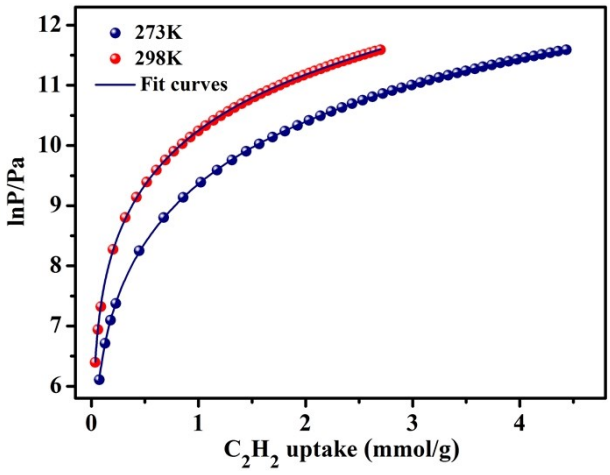


**(a)**

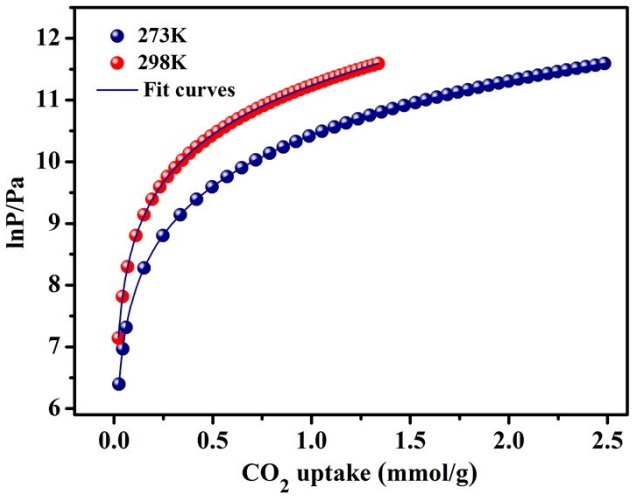


**(b)**

**Figure S9.** (a)Virial analysis of the $C_2H_2$ adsorption data at 298 K and 273 K for **3**. Fitting results: a0= -3438.80266, a1 = 642.98654, a2 =-90.36757, a3 =-0.09836, a4 = -1.78337, Chi^2 = 5.28472E-5, R^2 = 0.99997; (b) Virial analysis of the $CO_2$ adsorption data at 298 K and 273 K for **3**. Fitting results: a0= -2772.91188, a1 = -143.3409, a2 = 578.72905, a3 =-280.20604, a4 = -3.66184, Chi^2 = 1.64237E-5, R^2 = 0.99999.

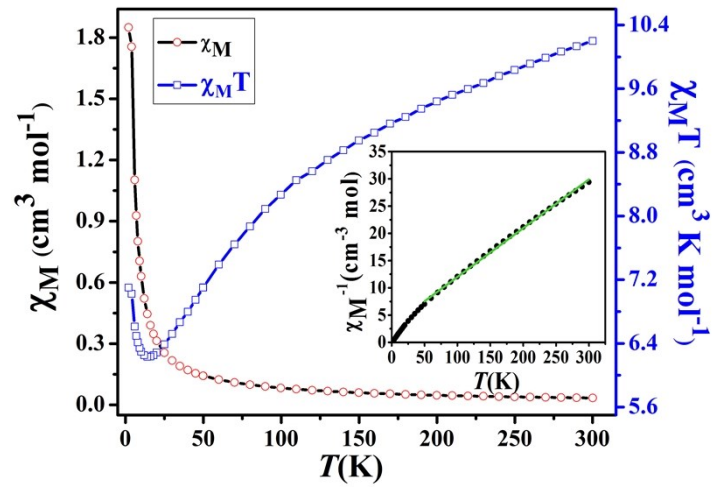


(a)

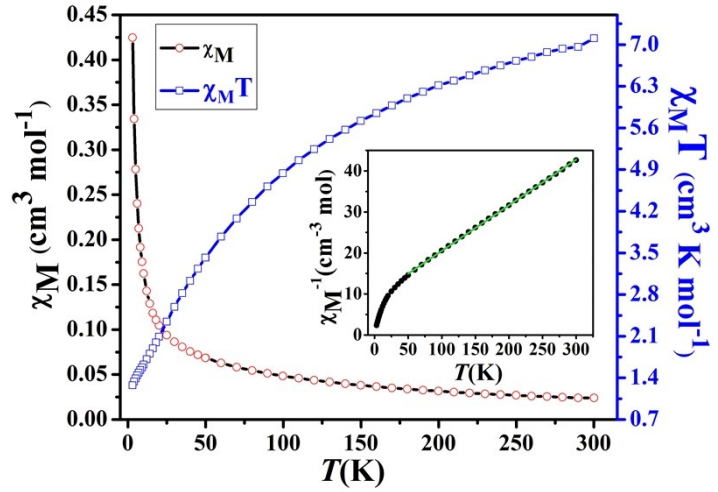


(b)

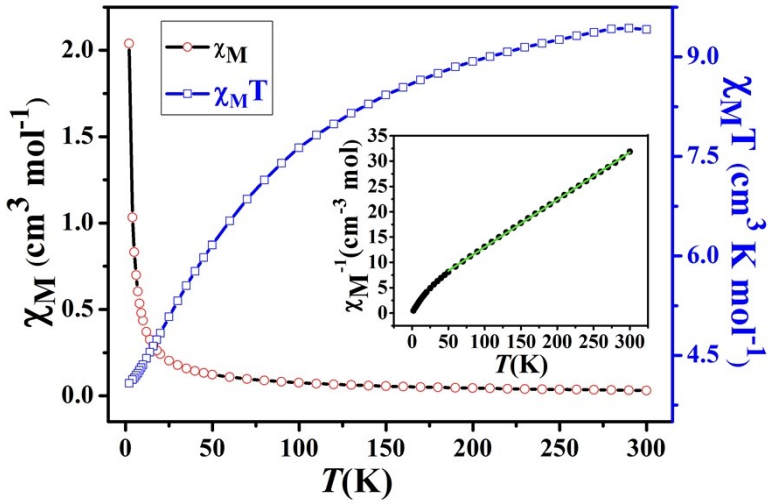


(c)

**Figure S10.** The $\chi_M T$, $\chi_M$, and $1/\chi_M$ vs. $T$ plots of **1-3 (a-c)**. The green line represents the best fit of the Curie-Weiss law.

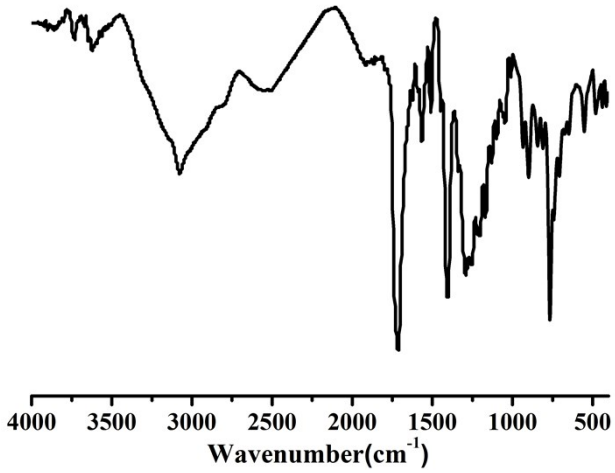


**(a)**

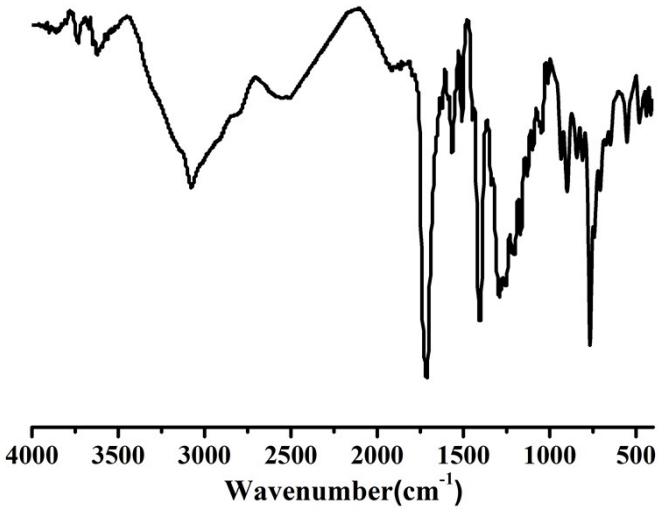


**(b)**

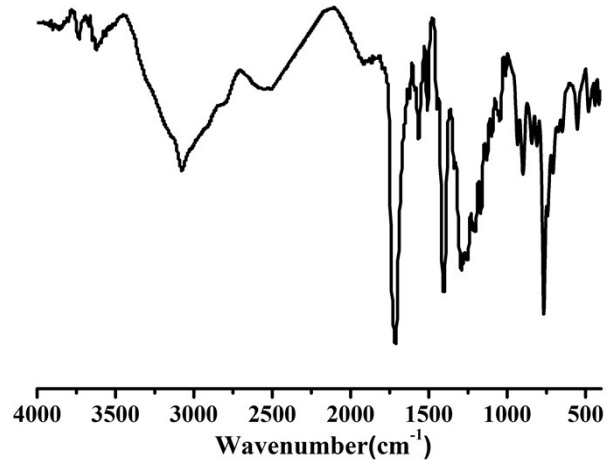


**(c)**

**Figure S11.** IR spectra of the as-synthesized **1-3** in (**a-c**).